VARIABLE ENERGY 2-MeV S-BAND LINAC FOR X-RAY AND OTHER APPLICATIONS

H. Bender, D. Schwellenbach, R. Sturges, and R. Trainham*,
National Security Technologies LLC, Los Alamos, NM 87544, U.S.A
J. Potter, JP Accelerator Works, Los Alamos, NM 87544, U.S.A.

Abstract

This paper describes the design and operation of a compact, 2-MeV, S-band linear accelerator (linac) with variable energy tuning and short-pulse operation down to 15 ps with 100-A peak current. The design consists of a buncher cavity for short-pulse operation and two coupled resonator sections for acceleration. Single-pulse operation is accomplished through a fast injector system with a 219-MHz subharmonic buncher. The machine is intended to support a variety of applications, such as x-ray and electron beam diagnostic development, and recently, electron diffraction studies of phase transitions in shocked materials.

INTRODUCTION

NSTec, LLC, provides support to the US National Nuclear Security Administration (NNSA) by operating the Nevada Test Site. For many decades the previous contractor, EG&G, operated a 20 MeV L-band linac at its Santa Barbara, CA location for diagnostic testing in support of the underground nuclear test program. This linac was decommissioned in the early 1990s and donated to Idaho State University. Over the last decade or so a need materialized for a low-energy short-pulse machine for diagnostic development. Fortunately, a spare 100-kV injector from the L-band linac still resided with us and it was deemed prudent to add an accelerating section to boost its energy. Our technical need was based on providing capability for x-ray scintillator characterization, Compton diode and gas Cerenkov detector impulse response measurements, radiation testing, low-energy radiography, and electron diffraction studies of phase transitions in shocked materials.

The paper is divided into three sections. First, we describe the design and layout of the machine. Second, results of initial commissioning and characterization are described. Third, preliminary studies on bremsstrahlung x-ray and electron diffraction [1] are presented as first use applications.

*NSTEC LLC, Special Technologies Laboratory, Santa Barbara, CA

LINAC DESCRIPTION

Accelerator and RF Systems

The main components of the new S-band linac consist of a fundamental buncher and a primary accelerator. A solid model view of these is shown in Figure 1. The fundamental buncher is a single-cavity, low-power structure. The primary accelerator is constructed in two sections with three cavities in the first (buncher-accelerator) and two in the second (variable-energy accelerator). The two sections are powered independently through the waveguides shown. The amplitude and relative phase of both sections can be varied to produce the desired output energy from 0.5 to 2.0 MeV. It should be noted that the maximum energy is actually limited by radiation control in the facility that houses the linac.

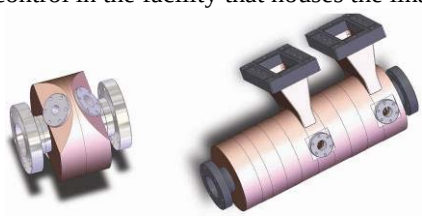

Figure 1. View of fundamental buncher (left) and primary accelerator (right).

Electrons are injected into the linac at 100 keV with pulse widths varying from 1 ns to several microseconds. A 219-MHz subharmonic buncher can compress the pulse to less than 300 ps for single-pulse operation.

Vacuum pumping of the structure is provided through the beam pipes at either end and internally through the beam apertures and resonator coupling slots. Because the structure is so short, this approach provides an adequate vacuum conductance. Cooling of the cavities is provided by conduction to the surrounding air.

Resonance control is maintained by tracking the frequency of the subharmonic buncher with the RF generator. The relative frequency of the S-band sections is maintained by slug tuners in each section (mounted on small flanges shown in Figure 1). A digital phase-locked loop adjusts the frequency of the RF generator and the position of the slug tuners to compensate for thermal drift. Figure 2 is a block diagram of the RF system with the phase-locked loops implemented.

The estimated power loss is 70 kW peak per resonator at full energy and the total power consumption is about 350 kW for the entire structure. At 3 A peak current in long-pulse mode (i.e., up to 4 μs), the beam power required at 1.5 MeV is 4.5 MW peak. Thus, the klystron power required is about 5 MW and is currently provided

by a CPI 5.5 MW unit. The fundamental buncher needs about 300 W of peak RF power for the drift space chosen. This power is supplied by an RF coupler which derives a modest amount of power from the klystron system.

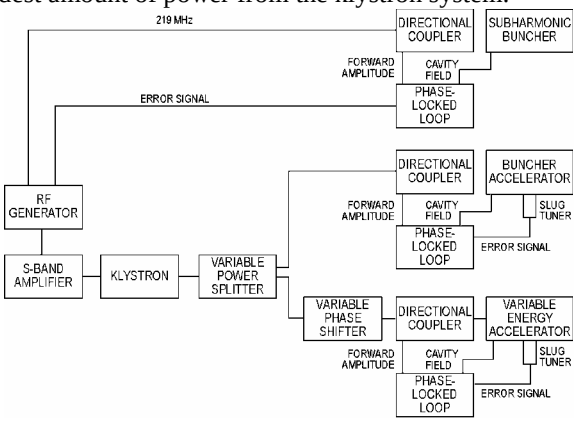

Figure 2: RF block diagram.

For variable energy operation, the RF power to the first section is held nearly constant while the amplitude and relative phase of the second section are varied. Figure 2 also shows the location of the adjustable RF power splitter and the high-power phase shifter. The few hundred watts of peak power required by the buncher are provided by a waveguide pick-off and the phase is set by a mechanical phase shifter.

As mentioned, an existing 219-MHz subharmonic buncher is used ahead of the fundamental buncher cavity for short-pulse operation. Future beam studies will determine whether an additional 714-MHz buncher will be required to obtain optimum single pulse capability. All required frequencies are generated by a Direct Digital Synthesizer chip. The chip is programmed to guarantee that all frequencies are locked in phase.

Beam Line Layout

The beam line is shown in Figure 3 with the described injector, buncher, and accelerator sections. Basic solenoid transport is used throughout the length of the beam line except for the end section which is presently configured for x-ray and electron diffraction experiments. The downstream section uses quadrupole triplet focusing magnets to provide small collimated spots on target and also imaging of diffraction patterns. The target chamber houses bremsstrahlung x-ray metal targets and/or thin foils for electron diffraction. The imaging chamber houses a phosphor screen.

BEAM MEASUREMENTS

Energy, Pulse Width, and Spot Size

Beam energy in short-pulse mode (1 ns) was measured with a 60-degree bend magnet spectrometer which was previously calibrated using a negative ion source [2]. This spectrometer was originally designed for use around 20 MeV, and thus magnet current was reduced considerably to just a few amps. However, reliable energy measurements were obtained in the range 0.7 MeV to 2.0 MeV and shown versus input RF power in Figure 4.

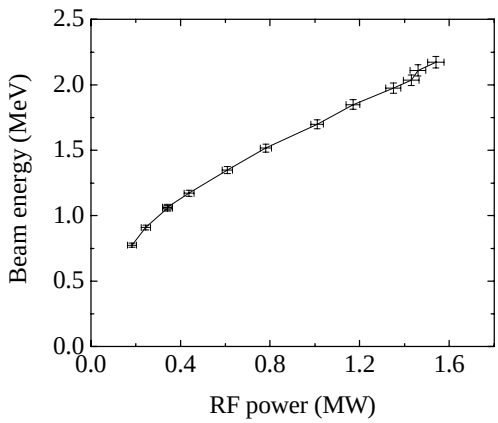

Figure 4: Beam energy measurement.

A plot of pulse width measured with a fast Faraday cup is shown in Figure 5. The injector pulse at approximately 1 ns and the RF modulation at 2.8 GHz is clearly seen. Individual pulses in the train are limited by the 80-ps Faraday cup response.

Spot size has been measured with phosphor screens at various locations along the beam line. At the 100-keV target shown in Figure 3 spot sizes are typically less than 5 mm. At the target chamber and imaging chamber in the downstream section, spot sizes are on the same order; however, some beam spreading is observed. This is presumably due to emittance growth caused by the accelerator cavities.

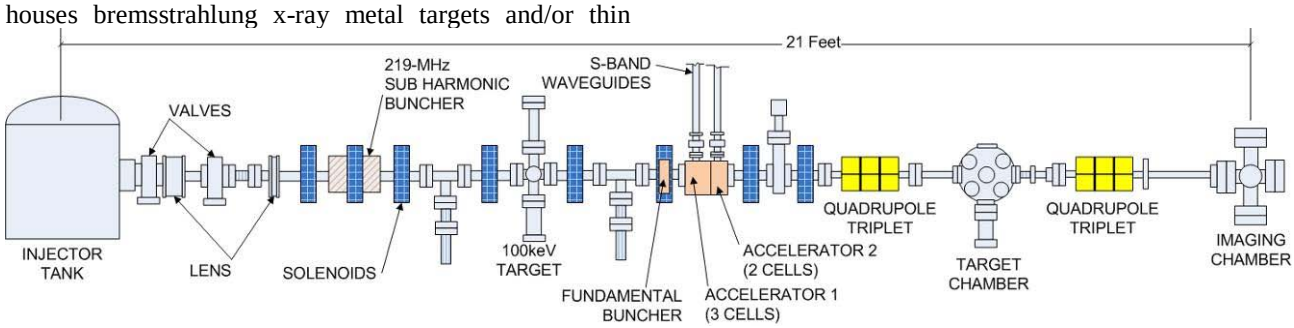

Figure 3: Accelerator and downstream configuration.

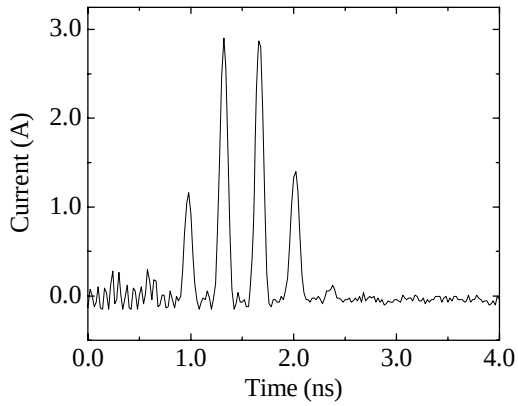

Figure 5: Pulse width measurement.

X-RAY AND ELECTRON DIFFRACTION STUDIES

One of the main uses of this accelerator is to provide bremsstrahlung x-rays for a variety of applications, as mentioned previously. Figure 6 shows a radiograph of a step wedge taken with the linac electron beam focused onto a tungsten target. Beam energy was approximately 0.5 MeV and pulse length was 1 ns.

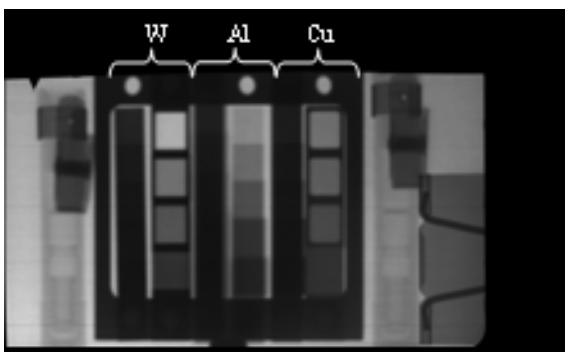

Figure 6: Bremsstrahlung x-ray step wedge radiograph.

One thousand pulses were integrated to record the image onto the Fuji phosphor imaging plate. Note the step wedge has two columns of downward increasing thickness each of W, Al, and Cu as shown. As a qualitative comparison of x-ray penetrating power, this radiograph was compared with another taken using a 0.4 MeV Marx bank x-ray source [3]. The transmitted intensity through the wedge was similar in both cases indicating roughly the same bremsstrahlung content. The accelerator was not opti-mized for minimum spot size for this particular test.

Another recent use of the machine has been relativistic electron diffraction as a phase transition diagnostic [1], the latter being important to equation of state studies for high-temperature and pressure physics. Preliminary simulations were completed to understand imaging diffraction rings in simple polycrystalline metals. For the diffraction simulations we used the Amaze series of codes from Field Precision [4]. Beam current distributions and emittances are produced by Gendist, and a separate C program uses the output from Gendist to generate the Bragg angle diffraction components. Magnum is used to model the beam line lenses and, finally, Omnitrack calculates the beam transport and emittance at the detector plane. Figure 7 shows the simulations for polycrystalline Al. With idealized zero emittance the modeled 4 indices (111), (200), (220), and (311) are clearly resolved. However, adding a reasonable emittance estimate of 0.3 π mm-rad causes broadening and smearing of the rings. Figure 7 also shows the image distortions introduced by the quadrupole lenses. Our initial diffraction experiments with an Al thin foil have indicated that beam emittance must be controlled precisely for high-fidelity imaging. Currently we are modifying the beam line to incorporate more collimation and better focusing for beam cleanup.

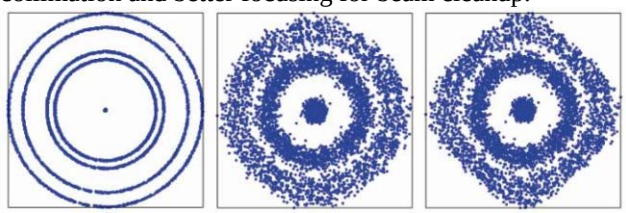

Figure 7: Electron diffraction simulations for polycrystalline Al. Quadrupole current is 0, 1, and 2 amps and emittance is zero, 0.3, and 0.3 π mm-rad respectively. Modeled diffraction indices are (111), (200), (220) and (311).

CONCLUSION

Initial operation and commissioning of the 2-MeV S-band linac is nearly complete with optimization underway. First applications for the linac have been bremsstrahlung x-ray production and experiments into electron diffraction for pump-probe studies of phase transitions. Future work includes enhanced beam emittance control, downstream tuning, and single short pulse operation down to 15 ps.

ACKNOWLEDGMENTS

The authors would like to thank C. Ekdahl and T. McCuistian of Los Alamos National Laboratory and N. Wilcox, W. Dreesen, C. Hollabaugh, and D. Morgan of NSTec for valuable technical support.

REFERENCES

[1] J.B. Hastings, F.M. Rudakov, D.H. Dowell, J.F. Schmerge, J.D. Cardoza, J.M. Castro, S.M. Gierman, H. Loos, P.M. Weber, Appl. Phys. Lett. 89 (2006) 184109.

[2] R. Trainham, A. Tipton, R. Bartsch, DOE/NV/25946-256 (2005).

[3] D. Morgan, D. Macy, M. Madlener, and J. Morgan, Flash X-ray Diffraction System for Fast, Single-Pulse Temperature and Phase Transition Measurements," PPPS'07, Albuquerque, June 2007, p. 209 (2007).

[4] For a description of the Amaze package see http://www.fieldp.com.